Supporting Information

for

Regioselective near-equatorial chlorination of C_s-$C_{70}(CF_3)_8$

A. A. Goryunkov, N. A. Samokhvalova, P. A. Khavrel, N. M. Belov, V. Yu. Markov,

L. N. Sidorov, and S. I. Troyanov

in

New Journal of Chemistry

Table of contents

Table S1. Schlegel diagrams, relative energies (at the DFT and AM1 levels of theory), and IUPAC lowest-locant indexes for isomers of $C_{70}(CF_3)_8Cl_2$ within 50 kJ mol^{-1} DFT energy gap. Filled and empty circles denote site of addition CF_3 groups and chlorine atoms

№	*Schlegel Diagrams of* $C_{70}(CF_3)_8Cl_2$	$\Delta\Delta_f H^o_0$ *kJ mol*$^{-1}$		*IUPAC name*
		DFT	*AM1*	
1	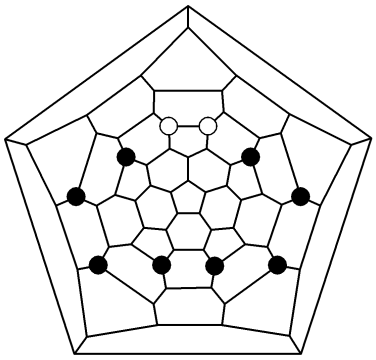	0.0	0.0	11,29-dichloro-1,4,19,41,49,60,66,69-octa(trifluoromethyl)-C_{70}
2	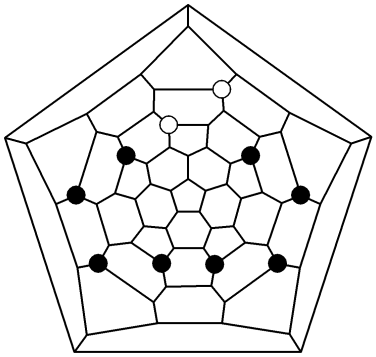	24.8	11.9	49,66-dichloro-1,4,11,19,31,41,60,69-octa(trifluoromethyl)-C_{70}
3	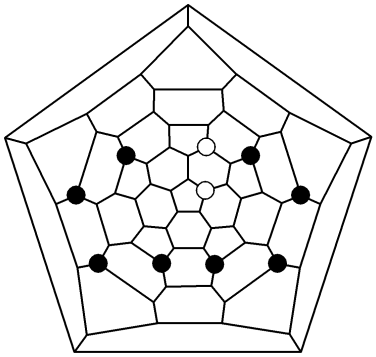	26.0	0.4	10,25-dichloro-1,4,19,41,49,60,66,69-octa(trifluoromethyl)-C_{70}

№	*Schlegel Diagrams of* $C_{70}(CF_3)_8Cl_2$	$\Delta\Delta_f H_0^o$ *kJ mol*$^{-1}$		*IUPAC name*
		DFT	*AM1*	
4	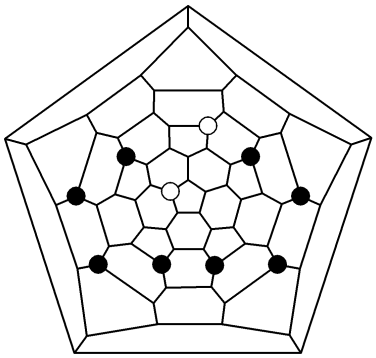	43.5	41.4	24, 61-dichloro-1, 4, 11, 19, 31, 41, 51, 64-octa(trifluoromethyl)-C_{70}
5	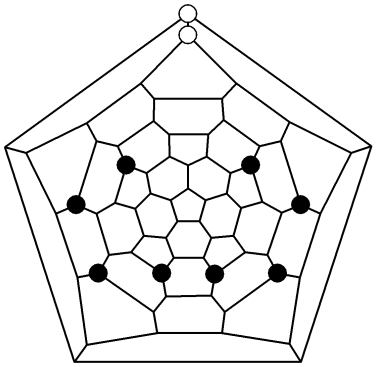	47.1	19.2	46,47-dichloro-1,4,11,19,31,41,60,69-octa(trifluoromethyl)-C_{70}
6	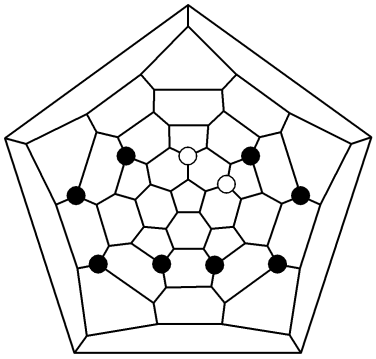	47.6	40.8	8, 27-dichloro-1, 4, 19, 41, 49, 60, 66, 69-octa(trifluoromethyl)-C_{70}

Table S2. Fragments of 3D projections of $C_{70}(CF_3)_8X_2$, X=H, Cl, Br, CF_3 , their relative DFT energies (within full set of corresponding isomers); some X...X, CF_2–F...X distances and C_{cage}–C_{cage}–C–F dihedral angles are given (DFT optimized geometries)

$C_{70}(CF_3)_8X_2$, X=	*DFT $\Delta\Delta_f H^o_0$ kJ mol^{-1}*	*Fragment of 3D Projection of $C_{70}(CF_3)_8X_2$*
H	0.0	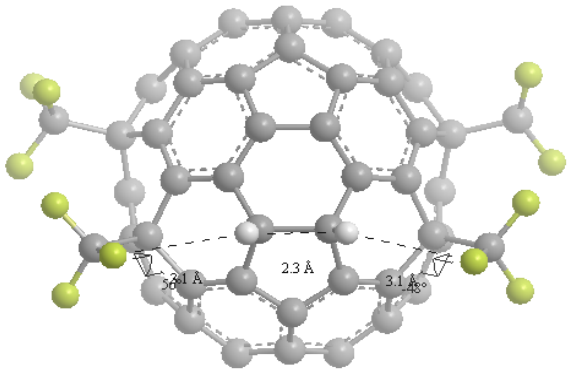
Cl	0.0	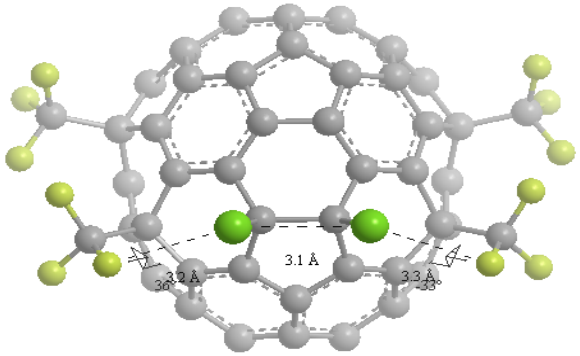
Br	0.0	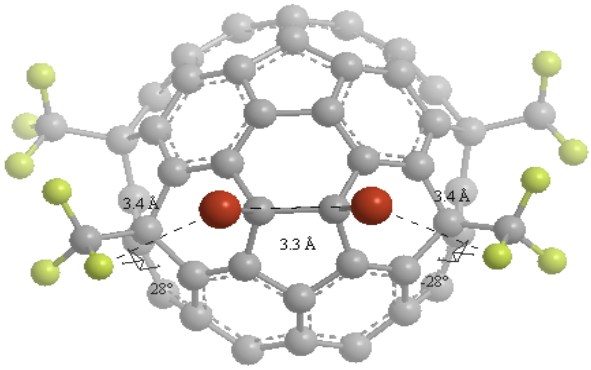
CF_3	12.0	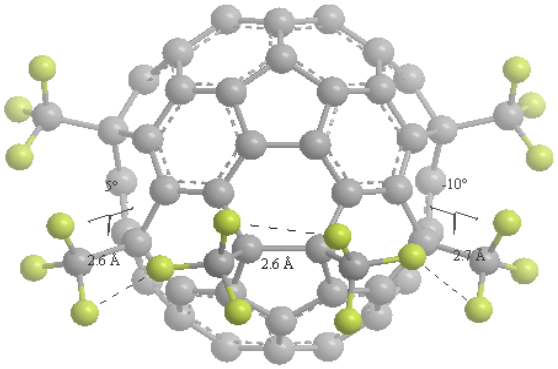

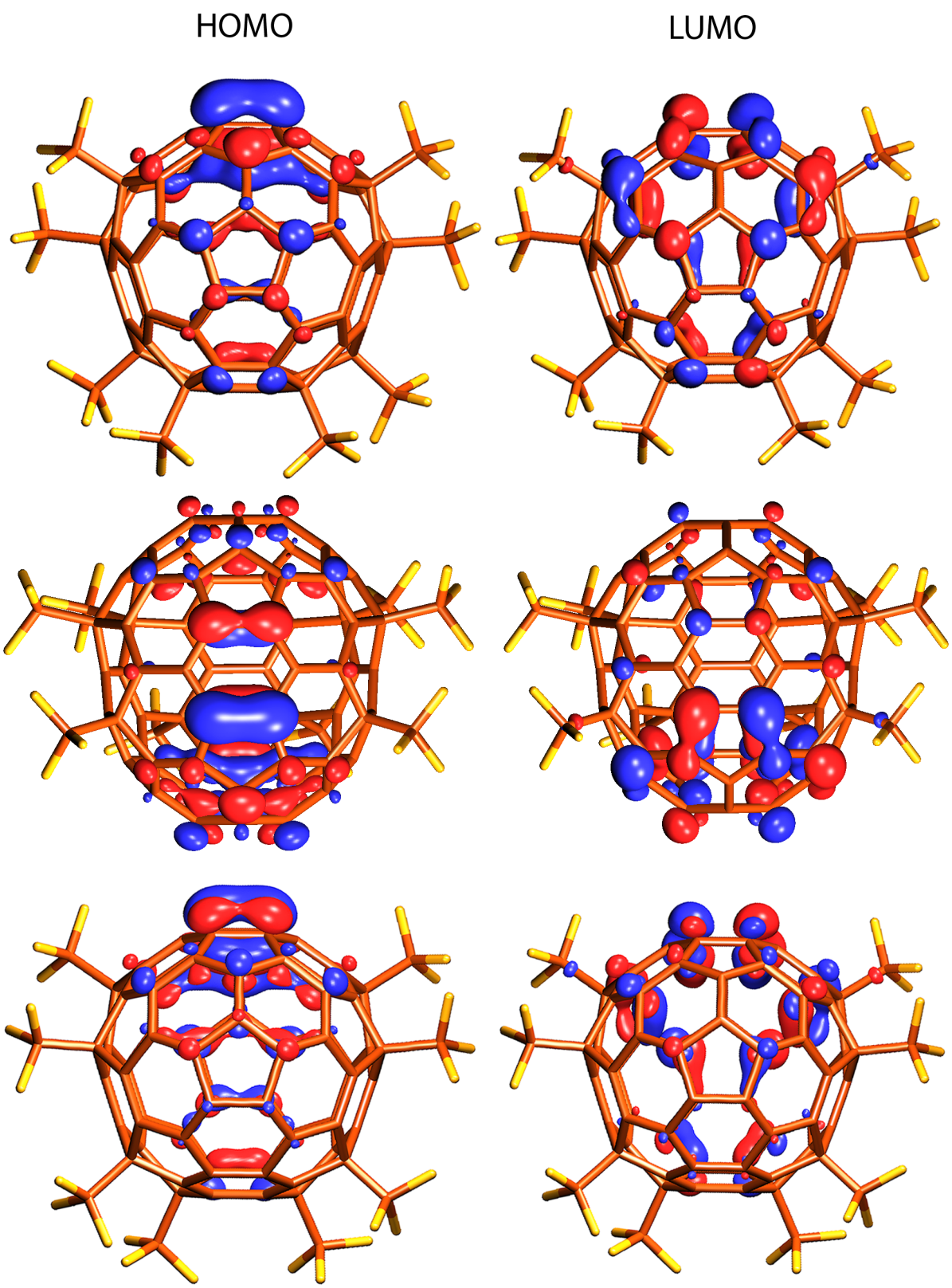

Figure S1. Top and side projections of probability isodensity surfaces (0.04) associated with HOMO (left) and LUMO (right) of C_s-$C_{70}(CF_3)_8$

Table S3. Possible radical $C_{70}(CF_3)_8Cl^{\cdot}$ intermediates within 40 kJ mol^{-1} DFT energy gap. Filled and empty circles denote sites of addition CF_3 groups and chlorine atom

№	Schlegel diagrams of $C_{70}(CF_3)_8Cl^{\cdot}$ intermediate	DFT $\Delta\Delta_f H^o_0$, kJ mol^{-1}
1	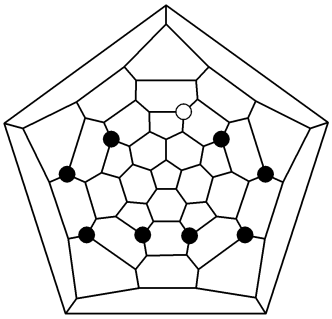	0.0
2	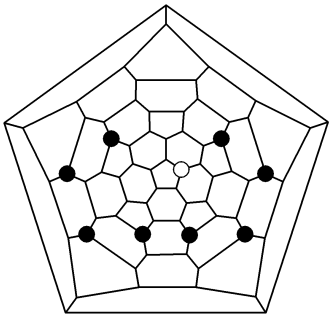	15.1
3	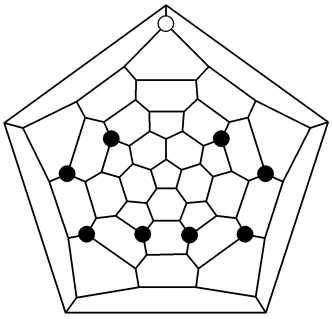	25.3
4	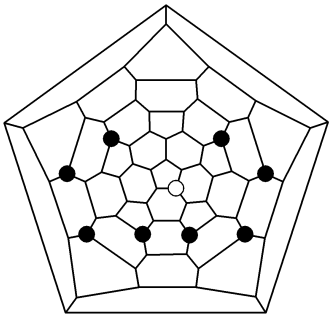	28.1
5	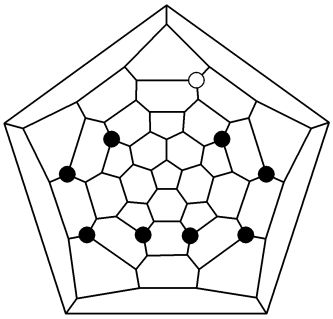	29.3
6	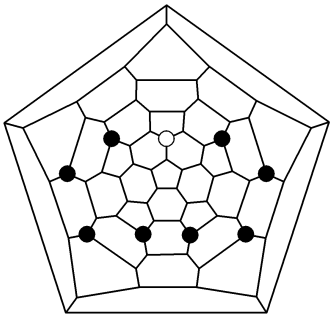	29.3
7	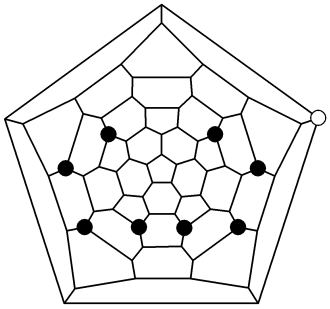	29.7
8	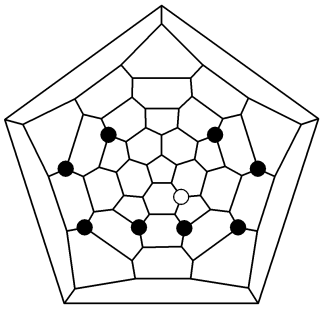	30.0

№	*Schlegel diagrams of $C_{70}(CF_3)_8Cl$ intermediate*	*DFT $\Delta\Delta_f H^o_0$, kJ mol^{-1}*
9	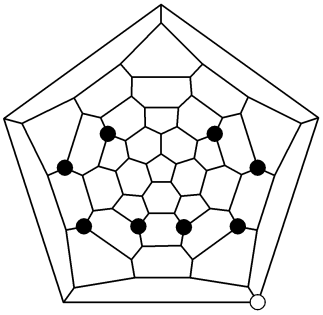	30.5
10	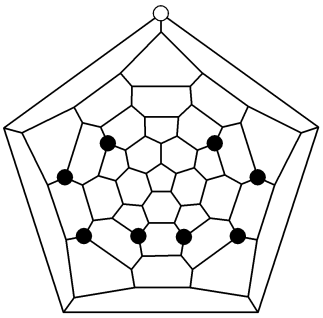	31.3
11	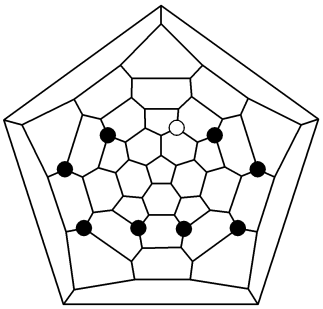	33.2
12	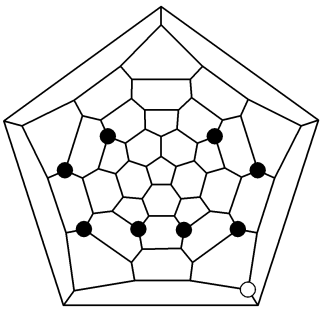	33.3
13	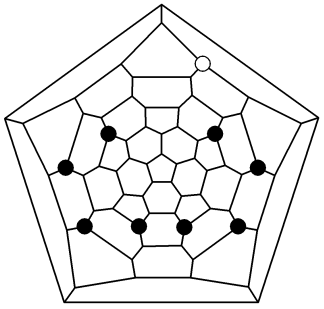	34.1
14	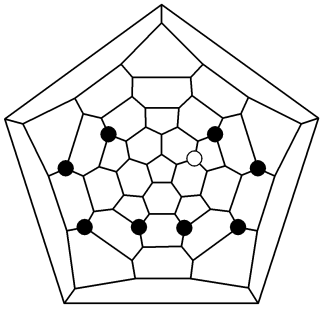	35.1
15	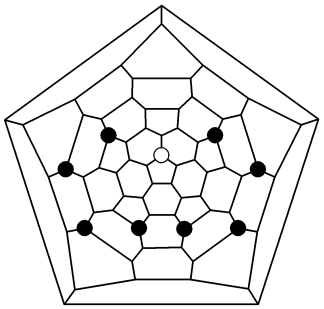	37.7
16	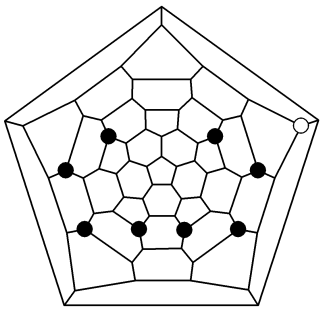	38.7

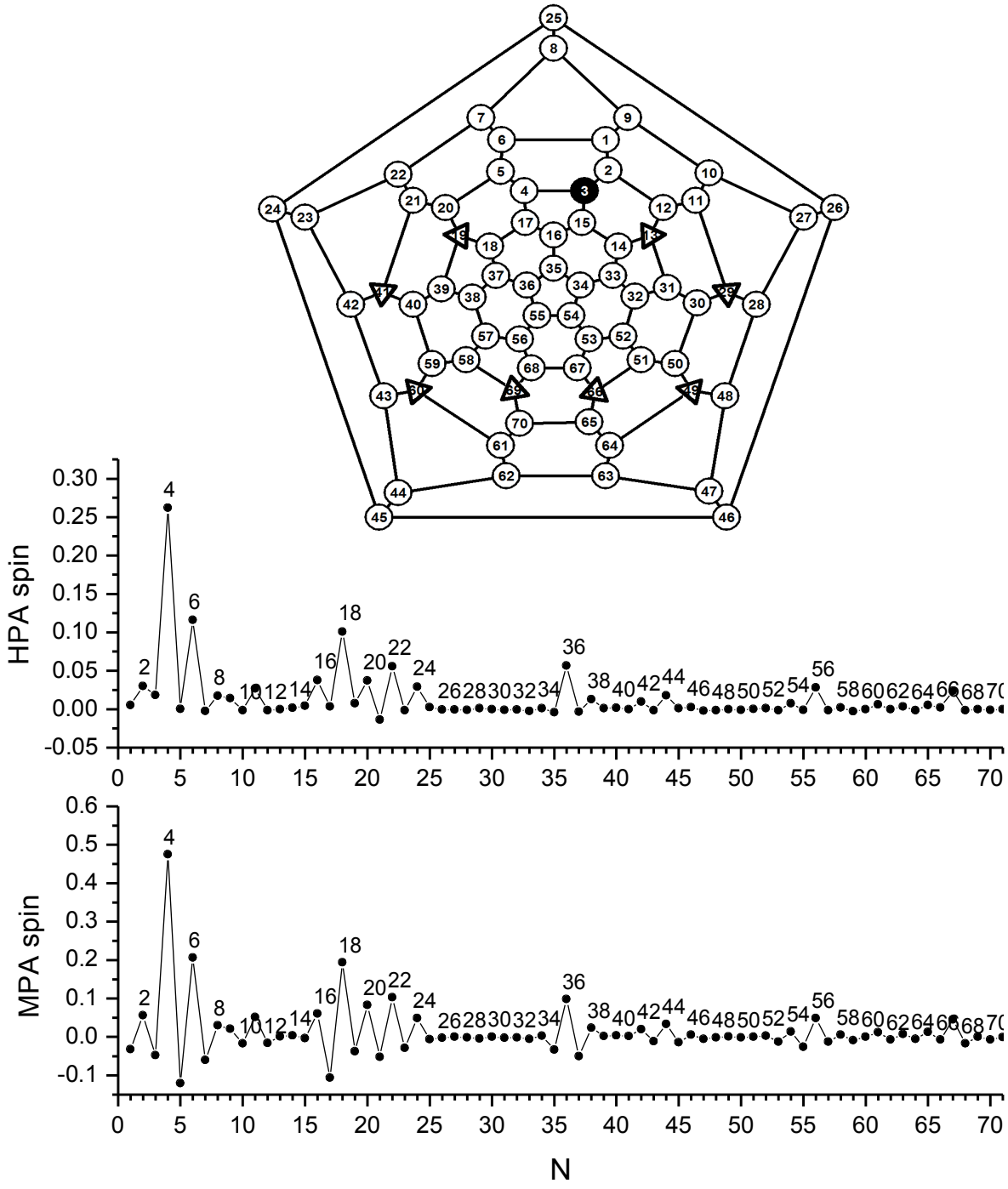

Figure S2. Mulliken and Hirshfeld population analyzes (MPA and HPA) of cage carbon atoms of the most energetic preferable radical intermediate $C_{70}(CF_3)_8Cl^{\cdot}$. Triangles and black filled circle denote sites of addition CF_3 groups and chlorine atom, correspondingly

Table S4. Experimental and calculated ^{19}F NMR chemical shifts in C_s-$C_{70}(CF_3)_8$ and C_s-$C_{70}(CF_3)_8Cl_2$

Assigns	***^{19}F NMR shifts -δF, ppm***			
	C_s-$C_{70}(CF_3)_8$		***C_s-$C_{70}(CF_3)_8Cl_2$***	
	Experimental	***Theoretical***	***Experimental***	***Theoretical***
Terminal CF_3	65.74		62.36	
Non terminal CF_3	61.68	59.16	61.67	61.11
	61.46	58.96	61.49	60.80
	61.40	58.47	61.44	60.68

[a] To bring theoretical scale in correspondence with the experimental one, quartets' positions in calculated spectra were set to those in experimental spectra.